

Fourth-order cascaded Raman shift in AsSe chalcogenide suspended-core fiber pumped at $2\ \mu\text{m}$

M. Duhant,^{1,*} W. Renard,¹ G. Canat,¹ T. N. Nguyen,² F. Smektala,³ J. Troles,⁴ Q. Coulombier,⁴
P. Toupin,⁴ L. Brilland,⁵ P. Bourdon,¹ and G. Renversez²

¹ONERA—The French Aerospace Lab, F-91761 Palaiseau, France

²Institut Fresnel UMR CNRS 6133, Université d'Aix-Marseille, Avenue Escadrille Normandie-Niemen, 13397 Marseille, France

³Laboratoire Interdisciplinaire Carnot de Bourgogne UMR CNRS 5209, Université de Bourgogne, 21000 Dijon, France

⁴Sciences Chimiques de Rennes, UMR CNRS 6226, Equipe Verres et Céramiques, Université de Rennes 1, 35000 Rennes, France

⁵Plate-Forme d'Etudes et de Recherche sur les Fibres Optiques Spéciales, 11 rue de Broglie, 22300 Lannion, France

*Corresponding author: mathieu.duhant@onera.fr

Received May 25, 2011; accepted June 25, 2011;
posted July 1, 2011 (Doc. ID 147971); published July 22, 2011

Cascaded Raman wavelength shifting up to the fourth order ranging from 2092 to 2450 nm is demonstrated using a nanosecond pump at 1995 nm in a low-loss $\text{As}_{38}\text{Se}_{62}$ suspended-core microstructured fiber. These four Stokes shifts are obtained with a low peak power of 11 W, and only 3 W are required to obtain three shifts. The Raman gain coefficient for the fiber is estimated to $(1.6 \pm 0.5) \times 10^{-11}$ m/W at 1995 nm. The positions and the amplitudes of the Raman peaks are well reproduced by the numerical simulations of the nonlinear propagation. © 2011 Optical Society of America

OCIS codes: 190.5650, 060.4370, 060.2390.

Chalcogenide glasses are remarkable not only for their strong optical nonlinear refractive index, which can be up to 800 times higher than in silica [1], but also for their large transparency extending far in the IR. Combining with the microstructure, one can make extremely nonlinear microstructured optical fibers (MOFs) [2]. These glasses are a good candidate for telecom applications such as signal regeneration [3], supercontinuum generation [4–6], and wavelength conversion in the IR using Raman shifting [7–9]. The Raman gain coefficient of chalcogenide fiber has already been measured at $1.55\ \mu\text{m}$ with typical values of $g_R = 2.3 \times 10^{-11}$ m/W for an AsSe step-index fiber (SIF) [8] and 5.7×10^{-12} m/W for an $\text{As}_{40}\text{Se}_2\text{S}_{58}$ SIF [7]. In [7], Kulkarni *et al.* observed a cascaded Raman wavelength shift (CRWS) up to three orders using a nanosecond source centered around 1550 nm with 350 W of peak power. The fiber core diameter was $6.5\ \mu\text{m}$, and the fiber length was 12 m. More recently, using a similar configuration, Ducros *et al.* obtained up to four CRWSs using 1 kW of peak power in a $10\ \mu\text{m}$ diameter core and 3 m long As_2S_3 SIF [9]. In this Letter, we report, for the first time to our knowledge, the observation of four CRWSs in an AsSe suspended-core MOF pumped around $2\ \mu\text{m}$ with only 11 W of peak power and of their quantitative modeling using the generalized nonlinear Schrödinger equation (GNLSE). We also measure the Raman gain coefficient around $2\ \mu\text{m}$.

In our study an $\text{As}_{38}\text{Se}_{62}$ MOF with a suspended core of $3.5\ \mu\text{m}$ diameter is used (Fig. 1). The fiber was fabricated using the casting method we have developed to prepare low-loss chalcogenide MOFs [10]. The losses are measured approximately to 0.8 dB/m at $1.55\ \mu\text{m}$. Using our finite element method software [11], the dispersion curve was obtained from the fiber profile captured by scanning electronic microscopy (SEM) and the glass refractive index was especially measured in the IR region in an $\text{As}_{38}\text{Se}_{62}$ prism. It gives a zero dispersion wavelength (ZDW) around $3.15\ \mu\text{m}$ (Fig. 1). This fiber is pumped with a gain-switched thulium-doped fiber laser using the

experimental setup shown in Fig. 2 [12]. The nanosecond pump source emits pulses with a central wavelength at 1995 nm. An isolator is used to prevent light reflections from the fiber cleave back to the laser. To improve the coupling efficiency to the chalcogenide fiber ($\sim 25\%$), a few centimeters of ultrahigh numerical aperture fiber (UHNA) are spliced after the isolator. The UHNA and the AsSe fiber are butt coupled using a splicer. Indium gallium alloy is deposited along the fiber to remove cladding modes. The output of the chalcogenide fiber is collected by a $100\ \mu\text{m}$ diameter multimode fiber into an optical spectrum analyzer up to 2400 nm.

In a first experiment, up to three CRWSs appear for a 4.4 m long MOF by varying the power [Fig. 3(a)]. Only 3 W of peak power is required to generate three shifts. The Stokes orders appear at wavelengths of 2092, 2205, and 2330 nm. By using a monochromator coupled to a liquid-nitrogen-cooled InSb detector, we could even observe a fourth Raman peak at 2450 nm for 1.7 m of fiber and an injected power of 11 W [Fig. 3(b)]. Because of injection stability and uncertainty in coupling efficiency, the peak power is known within 20% of error. Injection of 1995 nm nanosecond pulses into the AsSe fibers in the

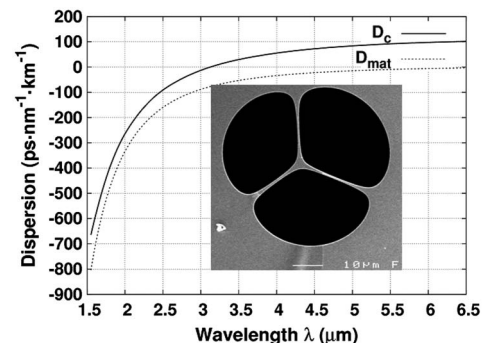


Fig. 1. Computed chromatic dispersion D_c of the fiber together with the material dispersion D_{mat} . (inset) Cross section of the fabricated fiber captured by SEM.

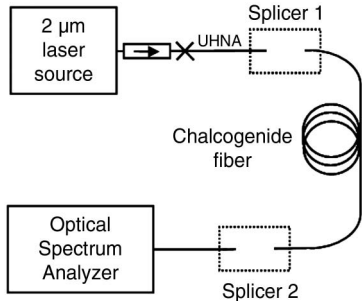


Fig. 2. Experimental setup for the Raman spectra.

normal dispersion regime leads to Raman scattering as modulation instability is prevented by dispersion and self-phase modulation is negligible for ns pulses. The CRWS occurring in this fiber at low peak power (2 W) indicates that the suspended-core structure considerably enhances the fiber nonlinearity and that the overall fiber losses are still low in the studied wavelength range. We observe a linear transmission by varying the injected peak power, which means that there is no two-photon absorption above $2\ \mu\text{m}$.

The modeling of the experiment has been performed using the GNLS [13] with the fourth-order Runge–Kutta in the interaction picture (RK4IP) method [14], the MOF linear properties obtained from the simulations (mode area $A_{\text{eff}} = 7.4\ \mu\text{m}^2 \pm 0.04\ \mu\text{m}^2$ at $2\ \mu\text{m}$, and dispersion), and the pulse parameters [Fig. 3(b)]. It is in good agreement with the experimental results. Numerical simulations using this method with a pump wavelength around $2\ \mu\text{m}$ and with stimulated Raman scattering has already been used for a tellurite MOF [15]. The nonlinear coefficient for As_2Se_3 is fixed to $1.3 \times 10^{-17}\ \text{m}^2/\text{W}$ [16]. To describe the Raman response, we start from the data provided by Ung and Skorobogatiy [17]. But we

determine a second set of optimized parameters ($\tau_1 = 22.5\ \text{fs}$, $\tau_2 = 225\ \text{fs}$, and $f_R = 0.132$) within 15% of the initial ones so as to reproduce all our experimental results and not only the first Raman peak of the recorded spectra. The simulations describe well the appearance of the Raman peaks and their central wavelengths as a function of the peak power. Nevertheless, their widths are slightly smaller than in the experimental results and the fourth Raman peak is not perfectly described. Several reasons may help to understand such differences. First, the studied suspended-core MOF is multimode in the considered wavelength range. Second, the exact Raman response of AsSe glass is not yet fixed accurately in the available literature (and the glass composition is $\text{As}_{38}\text{Se}_{62}$, not the usual As_2Se_3). Third, the fiber cross section is not strictly invariant along the fiber axis. Fourth, the temporal shape of the injected pulse is not a simple perfect secant hyperbolic like the one used in the simulations. Contrary to most other publications, we determine the modelling parameters with not only one Raman shift but with three or even four, and for many experiments. The estimated parameters are therefore more reliable.

To measure the Raman gain coefficient g_R , we use the same setup as we did previously (Fig. 2). Several curves are recorded corresponding to different injected peak powers ranging between 3 and 5 W. For this measurement, a 0.8 m long piece of our fiber is used. The output spectra were compared to a modeling of CRWS. We start from the Raman continuous equation given by [18] modified to take into account spectral and time-dependent intensity (the spectrum is divided in $N = 600$ bands λ_i , $i = 1, \dots, N$):

$$\frac{dA_i}{dz} = -\alpha A_i + \sum_{i,j} \varepsilon_{ij} \frac{g_R(\lambda_i, \lambda_j)}{A_{\text{eff}}} A_i |A_j|^2, \quad (1)$$

with

$$\varepsilon_{ij} = \begin{cases} -1 & \text{if } \lambda_i < \lambda_j \\ +\frac{\lambda_j}{\lambda_i} & \text{if } \lambda_i > \lambda_j \end{cases}, \quad (2)$$

where A_i is related to the total pump power by $P(t) = \sum_i |A_i(t)|^2$, α is the linear attenuation of the fiber, and A_{eff} is the mode area. The Raman gain, $g_R(\lambda_i, \lambda_j)$, is generated at λ_j by the pump λ_i . It has a Lorentzian spectral shape with an FWHM of 3 THz. The amplitudes A_i are initialized with quantum noise. The simulation results are in good agreement with the measured spectra for $g_R = (1.6 \pm 0.5) \times 10^{-11}\ \text{m/W}$ (see Fig. 4). Reference [8] gives a Raman gain coefficient of $2.3 \times 10^{-11}\ \text{m/W}$ at $1.56\ \mu\text{m}$ in a small core As_2Se_3 SIF. It is known that Raman gain coefficient scales inversely with the pump wavelength [13]. This would lead to a value of $1.8 \times 10^{-11}\ \text{m/W}$ at $2\ \mu\text{m}$ for the Raman gain coefficient for As_2Se_3 . Consequently, the value found for our $\text{As}_{38}\text{Se}_{62}$ suspended-core MOF is in good agreement with the literature.

In summary, we observed, for the first time to our knowledge, four orders of CRWSs in a suspended-core AsSe chalcogenide fiber pumped in normal dispersion regime at $2\ \mu\text{m}$ with an input peak power as low as 11 W. Light is shifted up to $2.45\ \mu\text{m}$. The positions and the

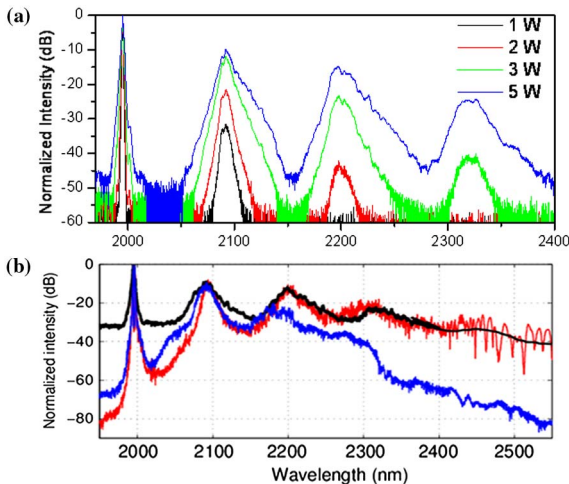


Fig. 3. (Color online) Cascaded Raman peaks in our AsSe suspended-core MOF. (a) Output spectra for different injected peak power up to 2400 nm in a 4.4 m long fiber. (b) Experimental data (black solid line) and simulation results with RK4IP method using data given in [17] for Raman response function (blue line) and using optimized parameters for this response (red line) in a 1.7 m long fiber and 19 W peak power. Experimental results above 2400 nm recorded with an InSb detector for 1.7 m long fiber.

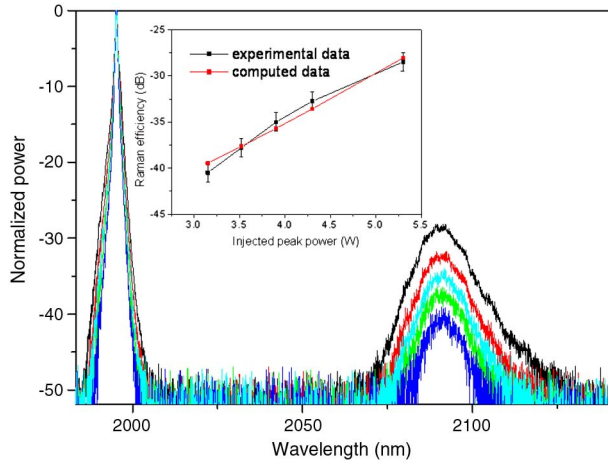


Fig. 4. (Color online) Evolution of the first Raman peak for different injected peak power in a 0.8 m long piece of our fiber. (inset) The Raman efficiency between the top of the pump peak and the top of the first Raman shift is plotted as a function of the injected peak power for experimental data (black line) and simulated data with $g_R = (1.6 \pm 0.5) \times 10^{-11}$ m/W (red line).

amplitudes of the Raman peaks obtained from numerical simulations of the nonlinear pulse propagation fit well the experimental data. We have also estimated the Raman gain coefficient to be $(1.6 \pm 0.5) \times 10^{-11}$ m/W around $2 \mu\text{m}$. This value is approximately 350 times larger than in silica fiber. Reducing further the core size will shift the ZDW around $2 \mu\text{m}$, so this AsSe MOF is a good candidate for supercontinuum generation in the mid-IR.

The authors want to thank French ANR (Confian), Délégation Générale pour l'Armement (DGA), and Région Ile de France for their financial support.

References

1. J. M. Harbold, F. Ilday, F. W. Wise, J. S. Sanghera, V. Q. Nguyen, L. B. Shaw, and I. D. Aggarwal, *Opt. Lett.* **27**, 119 (2002).

2. F. Désévéday, G. Renversez, L. Brilland, P. Houizot, J. Trolès, Q. Coulombier, F. Smektala, N. Traynor, and J.-L. Adam, *Appl. Opt.* **47**, 6014 (2008).
3. L. Fu, M. Rochette, V. Ta'eed, D. Moss, and B. Eggleton, *Opt. Express* **13**, 7637 (2005).
4. D. I. Yeom, E. C. Mägi, M. R. E. Lamont, M. A. F. Roelens, L. Fu, and B. J. Eggleton, *Opt. Lett.* **33**, 660 (2008).
5. M. El-Amraoui, J. Fatome, J. C. Jules, B. Kibler, G. Gadret, C. Fortier, F. Smektala, I. Skripatchev, C. F. Polacchini, Y. Messaddeq, J. Trolès, L. Brilland, M. Szpulak, and G. Renversez, *Opt. Express* **18**, 4547 (2010).
6. L. B. Shaw, R. R. Gattass, J. Sanghera, and I. Aggarwal, *Proc. SPIE* **7914**, 79140P (2011).
7. O. P. Kulkarni, C. Xia, D. J. Lee, M. Kumar, A. Kuditcher, M. N. Islam, F. L. Terry, M. J. Freeman, B. G. Aitken, S. C. Currie, J. E. McCarthy, M. L. Powley, and D. A. Nolan, *Opt. Express* **14**, 7924 (2006).
8. P. A. Thielen, L. B. Shaw, P. C. Pureza, V. Q. Nguyen, J. S. Sanghera, and I. D. Aggarwal, *Opt. Lett.* **28**, 1406 (2003).
9. N. Ducros, F. Morin, K. Cook, A. Labruyere, S. Février, G. Humbert, F. Druon, M. Hanna, P. Georges, J. Canning, R. Buczynski, D. Pysz, and R. Stepien, *Proc. SPIE* **7714**, 77140B (2010).
10. Q. Coulombier, L. Brilland, P. Houizot, T. Chartier, T.-N. N'Guyen, F. Smektala, G. Renversez, A. Monteville, T. Pain, H. Orain, J.-C. Sangleboeuf, and J. Trolès, *Opt. Express* **18**, 9107 (2010).
11. F. Zolla, G. Renversez, A. Nicolet, B. Kuhlmeiy, S. Guenneau, and D. Felbacq, *Foundations of Photonic Crystal Fibres* (Imperial College Press, 2005).
12. M. Jiang and P. Tayebati, *Opt. Lett.* **32**, 1797 (2007).
13. G. P. Agrawal, *Nonlinear Fiber Optics*, 4th ed. (Academic, 2007).
14. J. Hult, *J. Lightwave Technol.* **25**, 3770 (2007).
15. D. Buccoliero, H. Steffensen, O. Bang, H. Ebendorff-Heidepriem, and T. M. Monro, *Appl. Phys. Lett.* **97**, 061106 (2010).
16. G. Boudebs, S. Cherukulappurath, H. Leblond, J. Trolès, F. Smektala, and F. Sanchez, *Opt. Commun.* **219**, 427 (2003).
17. B. Ung and M. Skorobogatiy, *Opt. Express* **18**, 8647 (2010).
18. S. Yiou, P. Delaye, A. Rouvie, J. Chinaud, R. Frey, G. Roosen, P. Viale, S. Février, P. Roy, J. L. Auguste, and J. M. Blondy, *Opt. Express* **13**, 4786 (2005).